



HAL
open science

Augmented Reality Visualization Based On 3D Ultrasonography

Jun Shen, Nabil Zemiti, Oscar Caravaca Mora, Simon Antoine, Jean-Louis
Dillenseger, Philippe Poignet

► **To cite this version:**

Jun Shen, Nabil Zemiti, Oscar Caravaca Mora, Simon Antoine, Jean-Louis Dillenseger, et al.. Augmented Reality Visualization Based On 3D Ultrasonography. SURGETICA, Nov 2017, Strasbourg, France. lirmm-02105826

HAL Id: lirmm-02105826

<https://hal-lirmm.ccsd.cnrs.fr/lirmm-02105826v1>

Submitted on 21 Apr 2019

HAL is a multi-disciplinary open access archive for the deposit and dissemination of scientific research documents, whether they are published or not. The documents may come from teaching and research institutions in France or abroad, or from public or private research centers.

L'archive ouverte pluridisciplinaire **HAL**, est destinée au dépôt et à la diffusion de documents scientifiques de niveau recherche, publiés ou non, émanant des établissements d'enseignement et de recherche français ou étrangers, des laboratoires publics ou privés.

Augmented Reality Visualization Based On 3D Ultrasonography

Jun Shen^{1,2}, Nabil Zemiti², Oscar Caravaca², Simon Antoine¹, Jean-Louis Dillenseger¹, Philippe Pognet²

1. Inserm, U1099, Rennes, France; Université de Rennes 1, LTSI, Rennes, France;

2. LIRMM, Université de Montpellier, Montpellier, France

Contact: jun.shen@etudiant.univ-rennes1.fr

This paper presents an ultrasonography-based augmented reality guidance system. We achieved high accuracy of each calibration step and successfully made a visual guided robotic needle insertion experiment.

1 Introduction

Two main limitations in minimally invasive robotic surgery (MIRS) are the restricted field of view of the workspace and the lack of tactile and force feedback during the intervention. To compensate these limitations and provide complementary information, some MIRS bring ultrasonography (US) into the operating room to image the surgical area in real-time (e.g. [1] used US in transoral robotic resection of oropharyngeal tumors). This information can then be brought into the surgeon view by mean of augmented reality (AR) techniques to guide his/her gesture [2].

In this paper, we propose a simplified and easy to set up US-based AR guidance system. For this, we developed a new joint localization/calibration framework for the three-dimensional (3D) US probe based on an own-designed calibration phantom. This framework associated to stereoscopic camera allowed us to display the information from the US data to video-see-through display device (such as head-mounted display or a console viewer as in the da Vinci Surgical System). The usability of the whole system has been proved in a needle insertion experiment.

2 System overview

The objective was to display and overlay the preoperative information (e.g. a 3D model of the target as in Fig.1) to the stereo camera view. In the intraoperative stage, the target was localized by a calibrated 3D US device, as shown in Fig.1. Since the US probe was

calibrated with an attached position sensor (an active marker s), the spatial position and orientation of the US data were known in the coordinate system of the position sensor s , and so in the world coordinate system of the tracking system w . Meanwhile, the stereo camera c was also calibrated and localized according to w . This allowed us to register the preoperative information to the camera view. The two key points of this system were the US calibration/localization, and the camera-tracking system calibration.

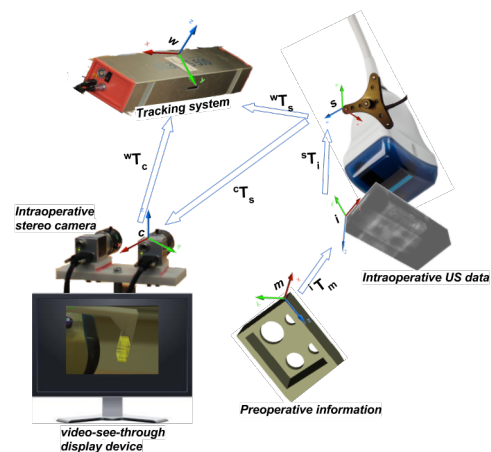


Figure 1: System overview of the augmented reality setup based on calibrated ultrasonography.

3 Ultrasound calibration

The objective of the calibration procedure was to determine a rigid transformation sT_i (Fig.1) between the position sensor attached on the probe and the US data.

The proposed calibration approach was based on an own-designed phantom with known geometrical properties, as depicted in Fig.2a. Compared to many conventional phantom-based methods using two references

(one for the probe and the other one for the phantom) [3] [4], there was only one reference s used in our design (Fig.2b). It greatly simplified the calibration procedure and highly improved the accuracy, because sT_i can be estimated by only a registration between the phantom in the acquired 3D US data and the phantom mesh model.

The setup of Fig.2b was placed into a water tank for US scanning, and the acquired data shown in Fig.3 was segmented. We generated a mesh model from the segmentation, and registered it to the model in Fig.2a with surface ICP registration method in 3D Slicer [5].

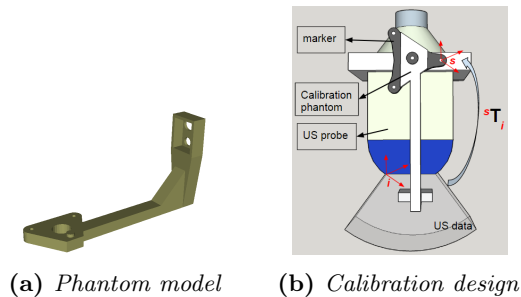


Figure 2: (a) calibration phantom mesh model; (b) calibration design: the phantom, the marker and the US probe were fixed together.

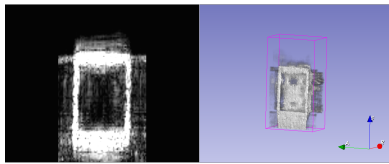


Figure 3: Acquired 3D US data.

4 Camera - tracking system calibration

A stereo camera was used for the 3D view, and it was calibrated by the classic chessboard-based method [6] with OpenCV [7]. Camera - tracking system calibration meant to determine the camera view in the world coordinate system w in Fig.1. For this, we used the marker s as common information between the camera and the world coordinate system w . The calibration problem can simply be solved by locating (currently manually) the position of the 4 LEDs of s in the stereo camera view. For the moment, this calibration is only valid when the tracking system and the camera are in a fixed pose. Hereby, we will attach a marker on the camera for tracking its movement in the future work.

5 Result and conclusion

Calibration setup: we used the tracking system Atracsys easyTrack 500 (0.1mm RMS at 1 meter distance) with

the Atracsys active marker (0.04mm RMS calibration error). The calibration phantom was printed by Stratasys Fortus 400mc 3D Printer with resolution 0.178mm. OpenCV estimated the calibration error of the stereo camera to be 0.28mm RMS. In order to estimate the influence of the human interaction for the camera-tracking system calibration, we asked 10 people for manually locating the 4 LEDs in the camera view. Compared to the real LEDs position, the highest error in the manually location estimation was 0.275mm. The accuracy of the 3D US probe calibration was estimated by the fiducial registration error (FRE) between the mesh model segmented from US data and the designed phantom model. In our experiment, the FRE was 0.86mm. We also estimated the error between the calibration phantom in the stereo camera view and its mesh model by comparing 4 pairs of vertices. The resulting RMS error was 1.971mm.

Needle insertion experiment: we used our guidance system to help to insert some needles into 11 holes of 1.5mm \varnothing in a plastic plane embedded in opaque gel (Fig.4a). The 3D model of the plastic plane was used as preoperative information which simulated the preoperative MRI/CT information in the real surgery scenario. In the intraoperative stage, we set the 3D US probe on the gel to image the plastic plane. This allowed us to locate the plastic plane and project its 3D model on the camera view (Fig.4b). The user inserted the needles according to the augmented information in the camera view. We performed first a set of 7 manual insertion experiments, and succeeded in 67 times out of 77 holes. Then, we simulated a robotic surgery scenario with the Raven II Surgical Robot holding the needles for insertion without force feedback. After several times practicing, the operator was able to insert the needles into most of the 11 holes by controlling the robotic arms.

In conclusion, we presented an US-based AR guidance system with high accuracy in the design and each calibration step. The needle insertion experiment shown the feasibility of the application in MIS scenarii.

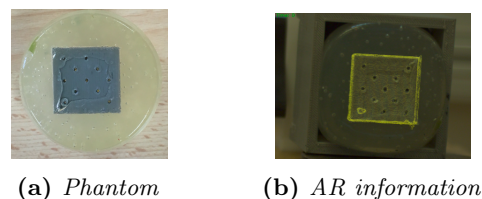


Figure 4: (a) target: a plastic plane with 11 holes embedded in gel; (b) augmented 3D mesh model of the plastic plane in the camera view.

6 Acknowledgement

This work was supported in part by the French ANR within the investissements d'Avenir Program Labex CAMI, ANR-11-LABX0004 and the Région Bretagne.

References

- [1] Clayburgh, D. R., et al. (2016). Intraoperative ultrasonography during transoral robotic surgery. *Annals of Otolaryngology, Rhinology and Laryngology*, 125(1):37-42.
- [2] Sauer, F., et al. (2001). Augmented reality visualization of ultrasound images: system description, calibration, and features. *Augmented Reality. Proceedings. IEEE and ACM International Symposium on. IEEE*, 30-39.
- [3] Lange, T., et al. (2011). Automatic calibration of 3D ultrasound probes. *Bildverarbeitung für die Medizin. Springer Berlin Heidelberg*, 169-173.
- [4] Lasso, A., et al. (2014). PLUS: open-source toolkit for ultrasound-guided intervention systems. *IEEE Transactions on Biomedical Engineering*, 61.10: 2527-2537.
- [5] Fedorov A., et al. (2012). 3D Slicer as an Image Computing Platform for the Quantitative Imaging Network. *Magn Reson Imaging*, 30(9):1323-41.
- [6] Zhang, Z., et al. (2000). A Flexible New Technique for Camera Calibration. *IEEE Transactions on Pattern Analysis and Machine Intelligence* 22(11):1330-1334.
- [7] Bradski, G., et al. (2008). Learning OpenCV: Computer vision with the OpenCV library. *O'Reilly Media, Inc.*